

Theoretical study of defect impact on two-dimensional MoS₂

Anna V. Krivosheeva^{1,†}, Victor L. Shaposhnikov¹, Victor E. Borisenko¹, Jean-Louis Lazzari², Chow Waileong^{3,4}, Julia Gusakova^{1,3}, and Beng Kang Tay^{3,4}

¹Belarusian State University of Informatics and Radioelectronics, P. Browka 6, 220013 Minsk, Belarus

²CNRS, Aix-Marseille Université, CINaM UMR 7325, Case 913, Campus de Luminy, 13288 Marseille Cedex 9, France

³NOVITAS, Nanoelectronics Centre of Excellence, School of Electrical and Electronic Engineering, Nanyang Technological University, 639798, Singapore

⁴CINTRA CNRS/NTU/THALES, Nanyang Technological University, 639798, Singapore

Abstract: Our theoretical findings demonstrate for the first time a possibility of band-gap engineering of monolayer MoS₂ crystals by oxygen and the presence of vacancies. Oxygen atoms are revealed to substitute sulfur ones, forming stable MoS_{2-x}O_x ternary compounds, or adsorb on top of the sulfur atoms. The substituting oxygen provides a decrease of the band gap from 1.86 to 1.64 eV and transforms the material from a direct-gap to an indirect-gap semiconductor. The surface adsorbed oxygen atoms decrease the band gap up to 0.98 eV depending on their location tending to the metallic character of the electron energy bands at a high concentration of the adsorbed atoms. Oxygen plasma processing is proposed as an effective technology for such band-gap modifications.

Key words: two-dimensional crystal; molybdenum disulfide; band gap; vacancy; oxygen

DOI: 10.1088/1674-4926/36/12/122002

EEACC: 2520

1. Introduction

Two-dimensional (2D) crystalline materials like graphene^[1], silicene^[2–4], and molybdenum disulfide (MoS₂)^[5] have recently attracted increased interest because of their electronic and optical properties which are attractive for new approaches of information processing at the nanoscale. Graphene and silicene demonstrate mainly metallic behavior leaving well studied semiconducting MoS₂ to be the most promising candidate for novel semiconductor-based nanoelectronic and nanophotonic devices. Its applicability in photovoltaic or photocatalytic elements^[5,6] or transistors^[5,7–10] has already been confirmed. Charge carrier mobility in the channel of field-effect transistors based on 2D MoS₂ was found to be comparable to that in thin silicon films or graphene nanoribbons^[11–13]. The transistors have a high on/off ratio (about 10⁸) and nearly ideal subthreshold swing (74 mV/dec). These features allow one to consider MoS₂ as a promising candidate for a digital switch. Monolayer MoS₂-based phototransistors show fast response (50 ms) and high photoresponsivity (7.5 mA/W)^[13]. Thickness-dependent photodetection has also demonstrated that monolayer and bilayer MoS₂ are sensitive to green light, while the trilayer is effective for red light detection^[8].

Bulk MoS₂ was experimentally reported to be a semiconductor with an indirect band gap (E_g) of 1.23–1.29 eV^[14,15], whereas a MoS₂ monolayer was described as a direct-gap semiconductor with a band gap of about 1.8 eV^[16]. According to the theoretical predictions in Reference [17], bulk MoS₂ is an indirect gap semiconductor with $E_g = 1.52$ eV, while monolayer MoS₂ has a direct gap of 1.72 eV. However, the fundamental band gap of few-layer MoS₂ cannot directly be obtained from optical experiments, as generally the optical

gap is smaller than the fundamental gap by the value of excitation binding energy. Nevertheless, experimental photoluminescence data of MoS₂ layers^[18] is consistent with the theoretical prediction of transition from indirect to direct band gap when going from multilayer to monolayer 2D MoS₂.

There were several attempts of band gap engineering in MoS₂. Its gap was found to be sensitive to an external electric field^[19] or biaxial strains^[17]. These approaches evidently have limited practical applications; a much more effective way of MoS₂ properties modification can be proposed through adsorption of adatoms and vacancy defect creation. Earlier, Huang and Cho^[20] investigated the adsorption of CO on a pure 1H-MoS₂ surface by using density-functional theory (DFT). Similarly, aromatic and conjugated compounds on MoS₂ were also studied^[21]. In Reference [22] the authors investigated adsorption of C, O, and Co atoms on MoS₂ nanoribbons and analyzed the impact of vacancies on the properties of the structure. In Reference [23] the adsorption of nonmetal elements like H, B, C, N, O, and F on the surface of MoSe₂, MoTe₂ and WS₂ nanosheets was studied, and the conditions of the appearance of local magnetic moment were determined. That information is important for the design of spintronic devices. In this paper, we present an alternative way of band gap engineering in MoS₂. We have theoretically analyzed the possibility of modification of electronic energy band structure of molybdenum disulfide by the presence of vacancies or oxygen atoms which are adsorbed or replace sulfur atoms, supposing that oxygen being isovalent to sulfur will perfectly substitute the later ones in the crystal lattice of MoS₂.

2. Computational details

The unit cell of bulk MoS₂ in hexagonal 2H phase (space

† Corresponding author. Email: anna@nano.bsuir.edu.by
Received 1 April 2015

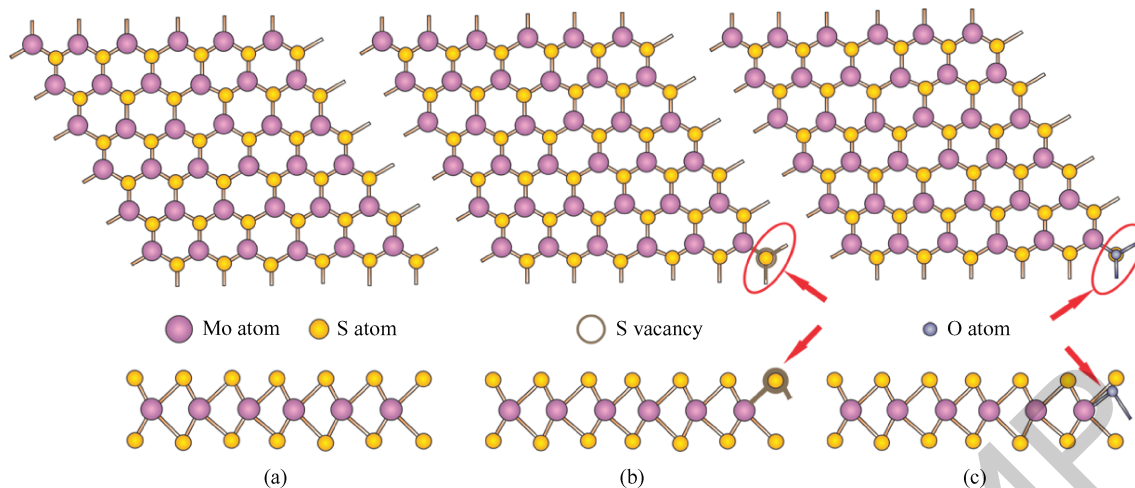


Figure 1. (Color online) Top and side view of layered MoS₂. (a) Undoped. (b) With S vacancy. (c) O-doped.

group P6₃/mmc) consists of two S–Mo–S layers, where Mo atoms of one layer are located on top of S atoms of the other layer, and vice versa. The layers are bonded to each other through Van-der-Waals forces. Each layer consists of two hexagonal planes of S atoms and an intermediate hexagonal layer of Mo atoms, thus each Mo atom is coordinated to six surrounding S atoms. In our calculations MoS₂ layered material was represented by a unit cell consisting of 1 S–Mo–S monolayer (ML). To study the defect formation, the unit cells with the translational symmetry from 2 × 2 up to 6 × 6 were used. The 6 × 6 cell for 1 ML is shown in Figure 1.

Full structural optimizations and total energy calculations within the DFT using the Vienna *ab initio* simulation package VASP^[24] with a plane-wave basis set were performed to simulate the stable atomic arrangements and electron energy band structures of pure and defected MoS₂ 2D structures. Projector-augmented wave (PAW)-type pseudopotentials of Perdew–Burke–Ernzerhof’s (PBE)^[25] within the generalized gradient approximation (GGA) or local density approximation (LDA) of Ceperly and Alder^[26] were used. For more accurate results 4p semi-core states of Mo were treated as valence. Additionally in order to determine the lattice constants and energy gap of bulk MoS₂ we have modeled its characteristics using vdW exchange functional, describing Van-der-Waals interaction, implemented in VASP code^[27]. Total energy minimization was achieved by calculation of Hellmann-Feynman forces and the stress tensor. The atomic relaxation was stopped when forces on atoms were less than 0.01 eV/Å. The energy cutoff of 520 eV was applied, while the 16 × 16 × 1 grid of Γ -centered points was used. The self-consistent procedure was continued until the difference between the total energies in two successive iterations was less than 1 meV/atom. A different vacuum width was approbated and 21 Å was finally found to be quite enough to suppress the influence of neighboring layers. For the band structure representation we have chosen up to 45 k-points for each segment along the high-symmetry directions of the hexagonal Brillouin zone.

We analyzed the influence of oxygen doping and oxygen adsorption as well as sulfur atom vacancies on the atomic arrangement and electron energy bands in MoS₂ layered structures. Oxygen is supposed to substitute sulfur in the lattice of

MoS₂ thus providing the formation of the MoS_{2–x}O_x ternary compound. The number of oxygen atoms (*x*) in the cells considered varies from 1 of 4 (25 at.%) for the 2 × 2 cell up to 1 of 72 (1.39 at.%) for the 6 × 6 cell.

3. Results and discussion

According to our calculations within the LDA approach taking into account the Van-der-Waals interlayer interaction, bulk MoS₂ was confirmed to be an indirect-gap semiconductor with a band gap of about 0.9 eV, that is somewhat lower than values extracted from other theoretical simulations^[17, 19] and experiments^[14, 15]. One should note, however, that fundamental band gaps obtained within the LDA approach should not be compared with experimental optical transition energies due to the excitonic effects^[28] and may be used mostly for qualitative analysis. Nevertheless, the structural parameters obtained with the vdW functional is much closer to experimental values than those obtained with pristine GGA or LDA approaches. The valence band maximum (VBM) is located at the Γ -point while the conduction band minimum (CBM) lies between the Γ and *K*-points that agrees well with the results, presented elsewhere^[19]. The calculations performed for pristine layered 2D MoS₂ have shown results close in general to the published data for this material. We have got the equilibrium in-plane lattice parameter *a* of 3.19 Å (GGA) and 3.12 Å (LDA) appropriately corresponding to the experimental *a* = 3.16 Å^[29]. The layered structure unlike bulk material behaves in a different way: VBM at the *K* point moves toward the Fermi level and occupies the same level as the Γ -point. Thus, the material behaves as a quasidirect gap semiconductor with the band gap of 1.86 eV.

The band structures of a single layer of undoped MoS₂ for a different number of translational cells are presented in Figure 2. The differences observed for 3 × 3 and 6 × 6 cells occur due to the symmetry of the hexagonal cell; however, the gap value remains unchanged.

Studying the effect of sulfur vacancies in MoS₂, we modeled their different concentrations by means of the unit cell translation. Figure 3 shows a series of energy band structures with one sulfur atom vacancy per cell. In the case of the en-

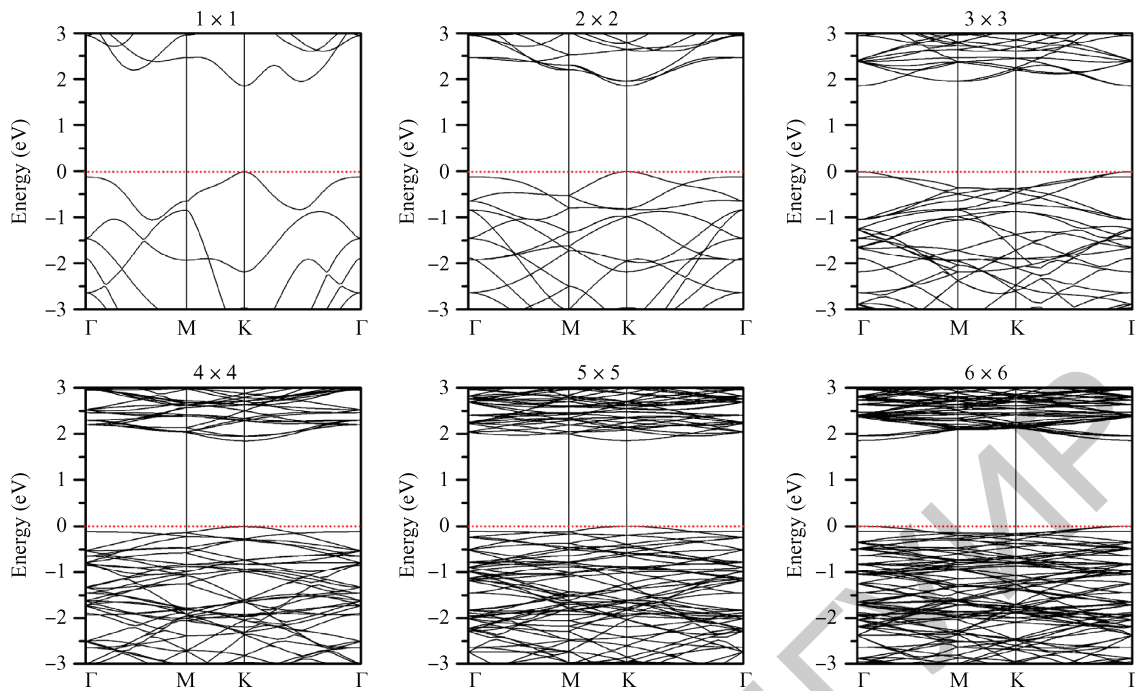


Figure 2. The energy band structures of MoS₂ single layer for a different number of translational cells. Zero at the energy scale corresponds to the Fermi level.

larged 2×2 supercells (the distance between the vacancies is about 6.12 \AA) new bands arise in the energy gap due to defect states, while the rest of the bands have practically the same dispersion except the upper valence band. The performed analysis of the density of states (DOS) shows that these bands are mainly formed by 4d-states of molybdenum atoms together with 3p-states of sulfur atoms, as it was already reported in Reference [30]. Additionally we found that only atoms neighboring a sulfur vacancy formed these additional bands. One sulfur vacancy in the 2×2 cell reduces the in-plane lattice constant a of MoS₂ from 3.120 to 3.002 \AA .

The formation energy of the vacancy, E_{vac} , was calculated by subtracting the total energy of the perfect structure from the sum of the total energy of a structure with a vacancy and the total energy of the missing atom in the vacancy defect. The total energy of the missing sulfur atom (i.e. its chemical potential) was determined from the bulk elemental phase. We obtained $E_{\text{vac}} = 2.8 \text{ eV}$, a positive value of which indicates an endothermic process of vacancy formation.

In the study of oxygen doping on the electronic properties of MoS₂, one sulfur atom from the top of the slab was replaced by an oxygen one and the atomic configurations were analyzed by varying the number of unit cells, thus obtaining different oxygen concentrations in MoS_{2-x}O_x ($x = 1/2, \dots, 1/4$).

As a result of structural optimization the crystal lattice of oxygen-doped MoS₂ remains practically unchanged. The oxygen atom preserves the in-plane position of the substituted sulfur atom while it moves closer to the neighboring Mo atom in the z direction. It results from the smaller S–O interatomic distance (2.77 \AA) as compared to the S–S one (3.13 \AA) and the Mo–O distance (2.08 \AA) as compared to the Mo–S one (2.42 \AA). The in-plane lattice parameter a of oxygen-doped MoS₂ is 3.13 \AA that is practically equal to the one for undoped MoS₂ (3.12 \AA).

The electron band structures presented in Figure 4 show that such substitution narrows the band gap in the case of the 2×2 cells, while the material changed to be an indirect-gap semiconductor. For the larger number of cells (starting from 3×3) the changes of the gap are insignificant. The changes in band structure also depend on oxygen concentration and the proximity of neighboring oxygen atoms. The closer oxygen atoms are located, the smaller is the energy gap. Small concentrations of oxygen atoms practically do not change the gap, whereas the 3×3 structure already demonstrates direct-gap behavior. The gap varies from 1.64 eV for 2×2 to 1.86 eV for 6×6 cells, which is practically the same as for pristine 2D MoS₂.

The analysis of partial densities of states for each case of substituting oxygen has shown that oxygen states do not give a sizable contribution; in all cases considered, the states in the proximity of the Fermi level are composed mainly by Mo 4d and S 3p electrons.

The changes in the band behavior occurring upon increasing the number of unit cells could be explained by the folding of the Brillouin zone for the hexagonal lattice. Nevertheless, the oxygen substitution of sulfur does not change the dispersion of the bands near the Fermi level, especially at the bands extrema. Thus, one can expect the carrier effective masses at the Γ -point and K -point, which are crucial for the transport properties of the material, to be practically the same as for the undoped material.

An effect of adsorption of oxygen atoms by the MoS₂ slab's surface was considered for up to 3×3 cells. As the surface of the slab is uniform, there are two possible positions of oxygen atom to be adsorbed: above one of the sulfur atoms (on top position) and in the center of the hexagon. In the second case the structural relaxation moved an O atom between molybdenum atoms (interstitial position). The first variant (O

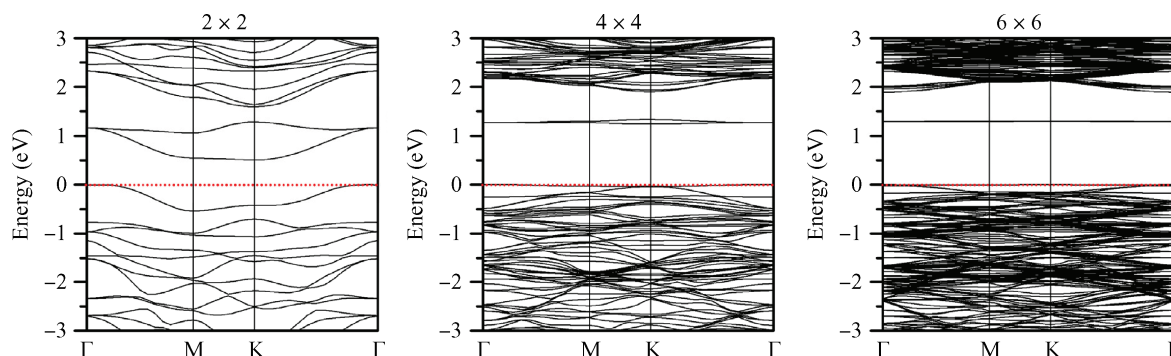


Figure 3. The electron energy band structures of MoS₂ single layer for a different number of translational cells with one sulfur vacancy. Zero at the energy scale corresponds to the Fermi level.

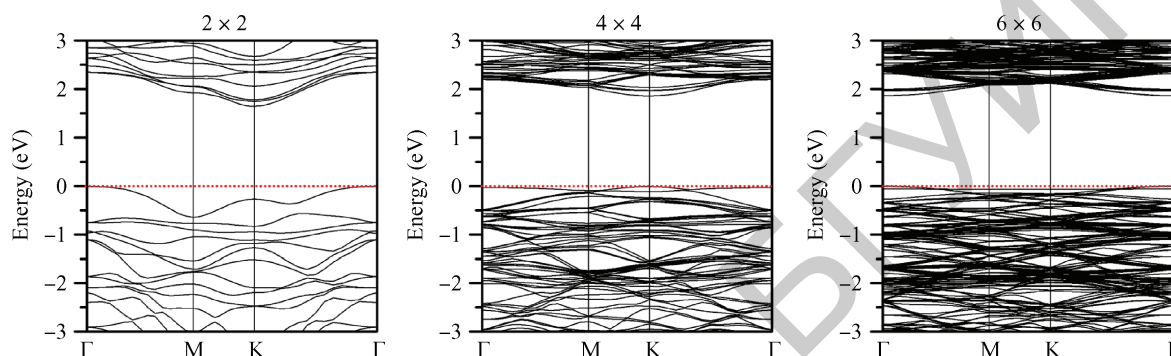


Figure 4. The electron energy band structures of MoS_{2-x}O_x supercells containing one oxygen atom for different number of translational cells. Zero at the energy scale corresponds to the Fermi level.

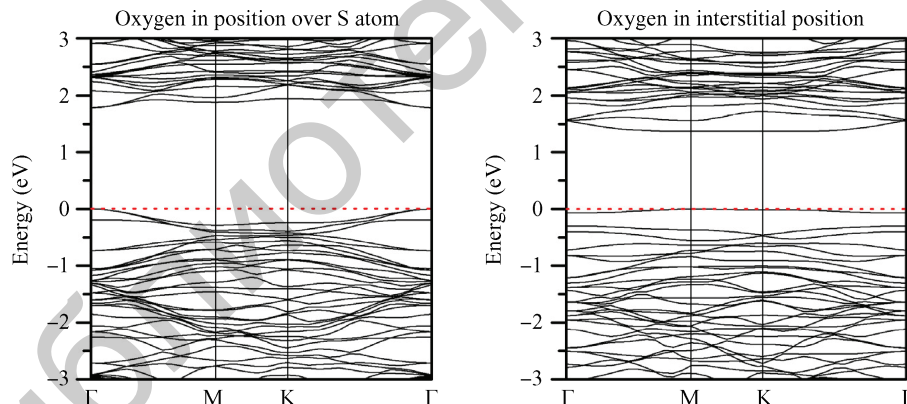


Figure 5. The electron energy band structures of MoS₂ single layer for 3 × 3 translational cell with one oxygen atom adsorbed over S atom, or as interstitial defect. Zero at the energy scale corresponds to the Fermi level.

atom above S atom) was found to be the energetically favorable case. Band structures, obtained for the 3 × 3 supercell, are presented in Figure 5. The reduction of the gap is observed for both cases, and becomes more pronounced when the oxygen atom occupies interstitial position. It is interesting to see that the adsorption of the oxygen atom on sulfur atoms reduces the gap slightly, up to 1.79 eV, whereas its location position in depth of the slab leads to gap reduction up to 1.37 eV.

The analysis of the total DOSs in MoS₂ and MoS_{2-x}O_x shows that the substitution of a sulfur atom by an oxygen one does not influence much DOS spectra, changing mainly the location of the peaks due to the changes in the band structures. The valence and conduction bands near the Fermi level in

MoS_{2-x}O_x are also mainly defined by 4d electrons of molybdenum with 2p electrons of sulfur. The O-2p electrons play an insignificant role, while all other states lie far from the region of interest.

When analyzing the DOS for the adsorbed oxygen (Figure 6) one can note strong changes of the band gap behavior upon increasing the cell size when an oxygen atom plays the role of an interstitial defect and less pronounced changes when oxygen is placed over a sulfur atom. In the first case when oxygen concentration is maximal the material behaves like a metal, increasing the gap up to 0.98 eV upon reducing the oxygen concentration (3 × 3 cell). In the case of adsorption on the top of the sulfur atom the material stays as a semiconductor with the

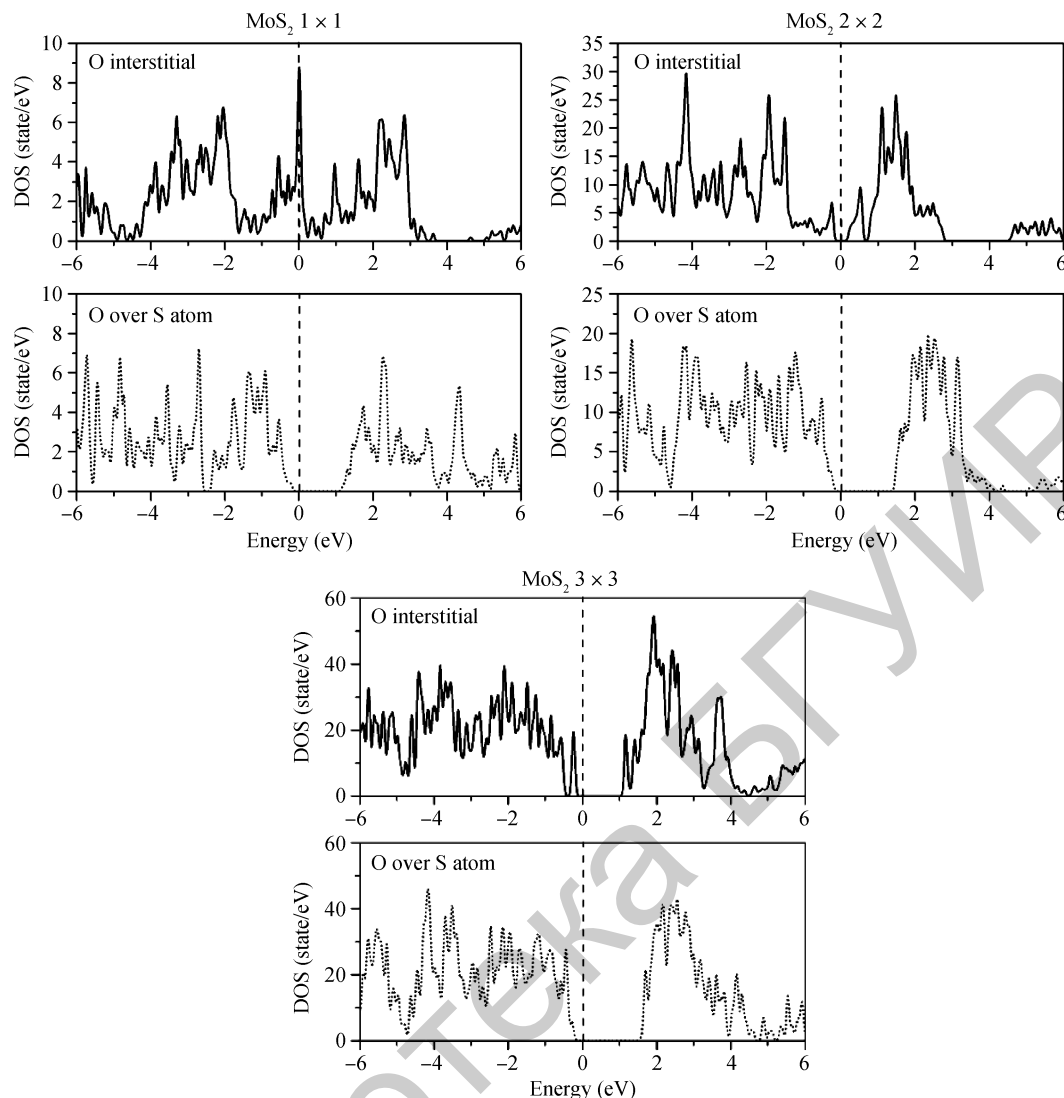


Figure 6. DOS of MoS₂ single layer with one oxygen atom adsorbed over S atom, or as interstitial defect for a different number of translational cells. Zero at the energy scale corresponds to the Fermi level.

gap increasing from 1.04 eV (1×1 cell) to 1.41 eV (3×3 cell).

4. Conclusions

The atomic structure and electronic properties of pure, defected and oxygen doped MoS₂ crystals analyzed with *ab initio* simulation confirm that, being an indirect-gap semiconductor with the energy gap of 0.9 eV for a bulk material, in the form of one monolayer 2D crystal it becomes a quasi-direct semiconductor; the energy gap in such a case increases up to 1.86 eV and its valence band maxima occurs either in the Γ -point or in the K -point. The replacement of sulfur atoms by oxygen ones does not disturb the stability of the crystalline structure of the matrix thus proving the formation of MoS_{2-x}O_x. Such doping narrows the band gap by approximately 0.22 eV with respect to an undoped material. Adsorption of oxygen atoms on top of sulfur ones slightly reduces the gap, whereas an oxygen atom located in the interstitial position has a more pronounced effect on the gap and at high concentrations transforms the host material into metal. A way of MoS₂ band gap modification by its processing in oxygen plasma is proposed to be an effective

tool for that^[31].

Acknowledgments

This work was supported by the Joint BRFFR-CNRS Project (No. F15F-003) and the Visby Program: scholarships for PhD studies and postdoctoral research in Sweden. The author is very thankful to Prof. N. V. Skorodumova for helpful discussions.

References

- [1] Geim A K, Novoselov K S. The rise of grapheme. *Nature Mater*, 2007, 6: 183
- [2] Lalmi B, Oughaddou H, Enriquez H, et al. Epitaxial growth of a silicene sheet. *Appl Phys Lett*, 2010, 97: 22310
- [3] Du Y, Zhuang J, Liu H, et al. Tuning the band gap in silicene by oxidation. *ACS Nano*, 2014, 8: 10019
- [4] Jamgotchian H, Colignon Y, Hamzaoui N, et al. Growth of silicene layers on Ag(111): unexpected effect of the substrate temperature. *J Phys: Condens Matter*, 2012, 24: 172001
- [5] Wang Q H, Kalantar-Zadeh K, Kis A, et al. Electronics and opto-

- electronics of two-dimensional transition metal dichalcogenides. *Nature Nanotech*, 2012, 7: 699
- [6] Liao J, Sa B, Zhou J, et al. Design of high-efficiency visible-light photocatalysts for water splitting: MoS₂/AlN(GaN) heterostructures. *J Phys Chem C*, 2014, 118: 17594
- [7] Wang H, Yu L, Lee Y H, et al. Integrated circuits based on bilayer MoS₂ transistors. *Nano Lett*, 2012, 12: 4674
- [8] Lee H S, Min S W, Chang Y G, et al. MoS₂ nanosheet phototransistors with thickness-modulated optical energy gap. *Nano Lett*, 2012, 12: 3695
- [9] Sarkar D, Liu W, Xie X, et al. MoS₂ field-effect transistor for next-generation label-free biosensors. *ACS Nano*, 2014, 8: 3992
- [10] Krasnozhan D, Lembke D, Nyffeler C, et al. MoS₂ transistors operating at gigahertz frequencies. *Nano Lett*, 2014, 14: 5905
- [11] Radisavljevic B, Radenovic A, Brivio J, et al. Single-layer MoS₂ transistors. *Nature Nanotech*, 2011, 6: 147
- [12] Kaasbjerg K, Thygesen K S, Jacobsen K W. Phonon-limited mobility in n-type single-layer MoS₂ from first principles. *Phys Rev B*, 2012, 85: 115317
- [13] Lopez-Sanchez O, Lembke D, Kayci M, et al. Ultrasensitive photodetectors based on monolayer MoS₂. *Nat Nanotech*, 2013, 8: 497
- [14] Kam K K, Parkinson B. Detailed photocurrent spectroscopy of the semiconducting group VIB transition metal dichalcogenides. *J Phys Chem*, 1982, 86: 463
- [15] Gmelin handbook of inorganic and organometallic chemistry. 8th ed. Berlin: Springer-Verlag, 1995, vol. B7
- [16] Mak K F, Lee C, Hone J, et al. Atomically thin MoS₂: a new direct-gap semiconductor. *Phys Rev Lett*, 2010, 105: 136805
- [17] Scalise E, Houssa M, Pourtois G, et al. Strain-induced semiconductor to metal transition in the two-dimensional honeycomb structure of MoS₂. *Nano Res*, 2012, 5: 43
- [18] Splendiani A, Sun L, Zhang Y, et al. Emerging photoluminescence in monolayer MoS₂. *Nano Lett*, 2010, 10: 1271
- [19] Ramasubramaniam A, Naveh D, Towe E. Tunable band gaps in bilayer transition-metal dichalcogenides. *Phys Rev B*, 2011, 84: 205325
- [20] Huang M, Cho K. Density functional theory study of CO hydrogenation on a MoS₂ surface. *J Phys Chem C*, 2009, 113: 5238
- [21] Moses P G, Mortensen J J, Lundqvist B I, et al. Density functional study of the adsorption and van der Waals binding of aromatic and conjugated compounds on the basal plane of MoS₂. *J Chem Phys*, 2009, 130: 104709
- [22] Ataca C, Sahin H, Aktürk E, et al. Mechanical and electronic properties of MoS₂ nanoribbons and their defects. *J Phys Chem C*, 2011, 115: 3934
- [23] Ma Y, Dai Y, Guo M, et al. Electronic and magnetic properties of perfect, vacancy-doped, and nonmetal adsorbed MoSe₂, MoTe₂ and WS₂ monolayers. *Phys Chem Chem Phys*, 2011, 13: 15546
- [24] Kresse G, Furthmüller J. Efficient iterative schemes for *ab initio* total-energy calculations using a plane-wave basis set. *J Comput Mater Sci*, 1996, 6: 15
- [25] Perdew J P, Burke K, Ernzerhof M. Generalized gradient approximation made simple. *Phys Rev Lett*, 1996, 77: 3865
- [26] Ceperley D M, Alder B J. Ground state of the electron gas by a stochastic method. *Phys Rev Lett*, 1980, 45: 566
- [27] Klimeš J, Bowler D R, Michaelides A. Van der Waals density functionals applied to solids. *Phys Rev B*, 2011, 83: 195131
- [28] Komsa H P, Krasheninnikov A V. Effects of confinement and environment on the electronic structure and exciton binding energy of MoS₂ from first principles. *Phys Rev B*, 2012, 86: 241201(R)
- [29] Böker T, Severin R, Müller A, et al. Band structure of MoS₂, MoSe₂, and α -MoTe₂: angle-resolved photoelectron spectroscopy and *ab initio* calculations. *Phys Rev B*, 2001, 64: 235305
- [30] Kadantsev E S, Hawrylak P. Electronic structure of a single MoS₂ monolayer. *Solid State Commun*, 2012, 152: 909
- [31] Chow L, Li H, Tay B K, et al. Oxygen doping of ultra-thin two-dimensional molybdenum disulfide. Abstract Booklet ICMAT13-A-3058 (M), 2013